
Permeability of heparinized hydrophilic polymer (H-RSD): Application to semipermeable membrane for microencapsulation of activated charcoal

Yuichi Mori, Shoji Nagaoka, Hiroshi Tanzawa, and Tetsuya Kikuchi

Basic Research Laboratory, Toray Industries Inc., 1,111 Teburo, Kamakura 248 Japan

Yosuke Yamada, Masaru Hagiwara, and Yasuo Idezuki

Department of Surgery, St. Marianna University School of Medicine

A series of heparinized hydrophilic polymers (H-RSD) composed of a hydrophobic element, a nonionic hydrophilic element, a cationic element and ionically bound heparin was synthesized. The permeability of the H-RSD polymers with various chemical compositions and water contents was investigated. From the studies on the permeability, it has been found that in order to maintain good permeability after heparinization, the nonionic hydrophilic element

is necessary. In addition, the microencapsulation of activated charcoal granules using a H-RSD polymer with a similar permeability to that of Cuprophane was examined. *In vitro* adsorption studies and *in vivo* direct hemoperfusion studies on the activated charcoal microencapsulated with the H-RSD polymer, show that the H-RSD coating prevents clot formation without loss of the absorption power of the activated charcoal.

INTRODUCTION

It is well recognized that the antithrombogenic membrane with appropriate permeability and proper mechanical strength is the most important element in the development of the blood purification system such as hemodialysis, hemofiltration and detoxification using adsorbents. In order to achieve antithrombogenicity, numerous synthetic materials have been developed and heparinized materials have been of special interest among them. However, from the view point of membrane permeability, few studies^{1,2} on the heparinized materials have been performed.

Expecting antithrombogenicity and good permeability, we have developed heparinized hydrophilic polymers (H-RSD) composed of a hydrophobic element (R), a hydrophilic element (S), a cationic element (D), and ionically bound heparin (H). Our previous studies³⁻⁶ have revealed that the excellent thromboresistance of these H-RSD polymers results from the continuous release of heparin effectively controlled by the compositions of hydrophilic and

cationic elements. To date, these polymers have been successfully applied to the medical devices such as catheters, A-V shunt tubes, ascites tubes, drainage tubes, and chambers of blood pumps.

In this article, we present our investigation of the permeability of the H-RSD polymers with varying chemical compositions and the application of the H-RSD polymers as semipermeable membranes in the microencapsulation of activated charcoal granules.

EXPERIMENTAL

Membrane preparation: The synthesis of the heparinized hydrophilic polymers (H-RSD) has been described in detail elsewhere.⁷ The commercially available terpolymer composed of 56 mol % vinyl chloride, 32 mol % ethylene, and 12 mol % vinyl acetate* was reacted with sodium *N,N*-diethyldithiocarbamate to introduce photosensitive dithiocarbamate groups. Then photoinduced graft copolymerization of methoxypoly(ethyleneglycol methacrylate) (SM) and *N,N*-dimethylaminoethyl methacrylate (DAEM) to the Graftmer R₃ containing dithiocarbamate groups was carried out. Subsequently, the *N,N*-dimethylaminoethyl groups of this graft copolymer were quaternized with ethyl bromide. The membranes for the measurement of permeability were fabricated by a dipping technique using a cyclohexanone/*N,N*-dimethylformamide solution of this cationic graft copolymer (RSD). Membrane thicknesses ranging from 50 to 200 μm were obtained by altering the dipping frequency of a cylindrical glassy mandril into the RSD solution (polymer concentration: about 6 wt %). The polymer coating was dried at 80 °C for 30 min to evaporate the solvents after each dipping and removed from the mandril by swelling in methyl alcohol. To extract the residual solvents, unreacted monomers and catalyzers, the membrane was soaked in methyl alcohol and subsequently in water at 60 °C for 1 to 2 days. Heparinization of the RSD membrane was conducted in 3 wt % sodium heparin aqueous solution at 60 °C for 2 days. Heparin was ionically bound to the quaternized *N,N*-dimethylaminoethyl groups of the RSD polymer. In the following discussion, this heparinized RSD polymer is referred to as the H-RSD polymer.

For comparison with the permeability of the RSD and the H-RSD membranes, the RD polymer was synthesized as follows: Only *N,N*-dimethylaminoethyl methacrylate (DAEM) was grafted to Graftmer R₃ containing dithiocarbamate groups and then the *N,N*-dimethylaminoethyl groups were quaternized with ethyl bromide. The preparation and heparinization of the RD membrane were carried out in the same manner as the RSD membrane. This heparinized RD polymer is called the H-RD polymer.

Microencapsulation procedure of activated charcoal: The activated charcoals used in the current study were the petroleum pitch base granules, LLP and MQ.[†] The charcoal granules were washed before using in ethyl alcohol for

* Graftmer R₃, The Japanese Zeon Co., Ltd.

† Taiyo Kaken Co. Ltd., surface area: 800–1200 m²/g, average diameter: 0.7 and 0.4 mm respectively.

20 min, filtered to remove carbon fines, and then dried. The activated charcoal granules (LLP and MQ), 150 g, were added to the cyclohexanone of 40 mL/ N,N-dimethylformamide of 40 mL/ethyl acetate of 120 ml solution of the RSD polymer of 200 mL with stirring. Subsequently, the RSD solution containing the charcoal granules was poured into a large quantity of distilled water with stirring to precipitate the RSD polymer on the surface of the charcoal granules. The thickness of the RSD coating layer was easily controlled by changing the polymer concentration of the RSD solution. To extract the residual solvents and unreacted monomers, the coated charcoal granules were washed in a large volume of distilled water and ethyl alcohol at 60 °C for 2 days. Then, the RSD coating layer was heparinized by soaking in a 2 wt % sodium heparin aqueous solution at 60° C for 1 day, and washed with distilled water for several times to remove free heparin and dried at room temperature in vacuum.

Measurement of permeabilities: In this study, water, sodium chloride and urea permeabilities were measured. The water permeability coefficient L_p is defined by

$$J_v = L_p \Delta P \quad (1)$$

where J_v and ΔP are the volume flux of water [$\text{cm}^3/(\text{cm}^2 \text{ s})$] and the pressure difference (dyn/cm^2) across the membrane respectively. L_p was measured using a batch filtering cell (membrane area 12 cm^2) and at a water head of 100 cm as ΔP .

The solutes (NaCl, urea) permeability coefficient P_2 is defined by

$$J_s = P_2 (\Delta C / \lambda) \quad (2)$$

where J_s , ΔC , and λ are the solute flux [$\text{mol}/(\text{cm}^2 \text{ s})$], the concentration difference (mol/cm^3) across the membrane and the membrane thickness, respectively. P_2 was measured by using a batch dialyzer shown schematically in Figure 1. The measuring operations for P_2 were as follows: The NaCl or urea solution and pure water were placed into the concentrate compartment and the diluent compartment, respectively. Both compartments were stirred from 30 min to 3-h, depending on the permeability of the membrane. The diluent was sampled and the NaCl concentration was analyzed by electric

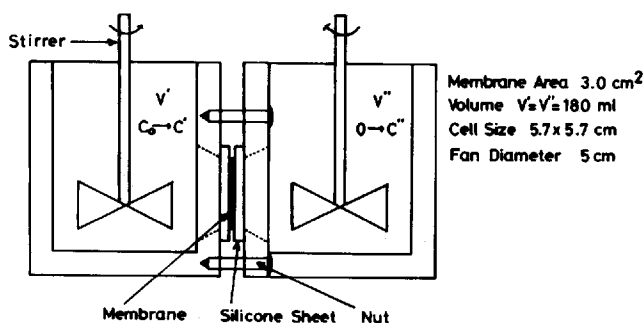


Figure 1. Schematic diagram of batch dialyzer for measuring solute permeability.

conductometry and the urea concentration was analyzed by spectrometry using *p*-dimethylaminobenzaldehyde as a colorant. The coefficient P_2 was calculated by eq. (3), which is the integrated form of Eq. (2):

$$P_2 = \frac{2.303 \lambda V''}{[1 + (V''/V')A_t]} \log_{10} \frac{C_0}{C_0 - \left(1 + \frac{V''}{V'}\right)C_t} \quad (3)$$

where V' , V'' , A , C_0 , and C_t are the volumes of the concentrate and the diluent compartment, the effective membrane area, the initial concentration of the concentrate, and the concentration of the diluent at sampling time t , respectively. The rate of stirring was investigated beforehand by changing the revolution rate. The stirring rate was greater than 900 rpm, where the boundary resistance is negligible. Measurements of L_p and P_2 were conducted at $30 \text{ }^\circ\text{C} \pm 1 \text{ }^\circ\text{C}$ by placing the cell in an air oven.

In vitro adsorption studies: The dry activated charcoal granules, 0.1 g, were added to creatinine and uric acid solutions of 30 mL with stirring. The compositions of the creatine and uric acid solutions are as follows: Na^+ 132 meq/L, K^+ 2 meq/L, Ca^{++} 2.5 meq/L, Mg^{++} 1.5 meq/L, Cl^- 105 meq/L, CH_3COO^- 33 meq/L, glucose 200 mg/dL, creatinine 8 mg/dL, and uric acid 6 mg/dL. The adsorption studies were conducted at $37 \text{ }^\circ\text{C}$. One ml samples were taken at various times and the creatinine and uric acid concentrations in each sample were measured by spectrometry using picric acid and phosphotungstic acid as colorants, respectively.

In vivo studies: The extracorporeal circuit composed of a roller pump, a drip chamber and a cartridge containing activated charcoal granules of 50 g were placed between the femoral artery and vein of mongrel dogs weighing 11 to 14 kg. Intravenous sodium pentobarbital was used as anesthesia. The priming volume of the extracorporeal circuit was about 100 mL and the blood flow was about 200 mL/min. The direct hemoperfusion was initiated within 5-min after intravenous injection of 50 mL of a physiological saline solution of creatinine (2 wt %) and sodium heparin, 1 mg/kg. Blood samples of 20 mL were taken at various times and the creatinine concentration in each sample was analyzed by spectrometry using picric acid as a colorant. In addition, the pressure drop between the inlet and outlet of the cartridge of the activated charcoal was continuously monitored.

Scanning electron microscopic studies: The surface and the cross section of the coated and uncoated activated charcoal granules were coated with gold in a vacuum evaporator and examined in a scanning electron microscope (Hitachi-Akashi MSM-4). The cross section was prepared by cutting a charcoal granule adhered to adhesive tape by a razor under a microscope.

RESULTS

Permeabilities of the heparinized hydrophilic polymers (H-RSD): The feeding monomer composition, water content, water permeability (λL_p) and the NaCl and urea permeabilities (P_2) of five species of RSD and H-RSD polymers are

summarized in Table I. For control, the water content and permeability of Cuprophan, a commercially available cellulosic membrane are also shown in Table I. In addition, similar data for the three species of RD and H-RD polymers are summarized in Table II for comparison with the RSD and H-RSD membrane.⁵ The heparin contents of the H-RSD and H-RD polymers were gravimetrically analyzed and ranged from 10 to 15 wt % irrespective of varying feeding compositions of the DAEM monomer.

Figures 2, 3, and 4 demonstrate the effects of the water content of the membranes on the water, NaCl, and urea permeabilities, respectively. As a matter of course, the water, NaCl, and urea permeabilities monotonically increase with the water content of the membrane.

In addition, it was found that the permeability of the Cuprophan is on the correlation curves of the H-RSD membrane. On the basis that Cuprophan has

TABLE I
Feeding Monomer Composition, Water Content, and Permeability of RSD and H-RSD Membrane

Sample No.	Feeding Composition (wt %)			Water Content (wt %)	λL_p ($\text{g}^{-1} \text{cm}^3 \text{s}$)	P_2 (NaCl) ($\text{cm}^2 \text{s}^{-1}$)	P_2 (Urea) ($\text{cm}^2 \text{s}^{-1}$)
	Graftmer-R ₃	SM	DAEM				
RSD-1	55.6	12.3	32.1	42.2	1.3×10^{-13}	5.7×10^{-7}	2.7×10^{-6}
RSD-2	44.6	29.7	25.7	46.5	1.6×10^{-13}	8.8×10^{-7}	3.2×10^{-6}
RSD-3	42.5	33.0	24.5	57.5	4.5×10^{-13}	1.9×10^{-6}	4.7×10^{-6}
RSD-4	26.3	58.5	15.2	66.6	7.2×10^{-13}	3.4×10^{-6}	6.1×10^{-6}
RSD-5	19.1	69.9	11.0	80.3	13.2×10^{-13}	6.1×10^{-6}	9.7×10^{-6}
H-RSD-1 ^a	—	—	—	16.7	N.T. ^b	1.4×10^{-7}	6.2×10^{-7}
H-RSD-2	—	—	—	27.3	N.T.	2.8×10^{-7}	9.4×10^{-7}
H-RSD-3	—	—	—	34.7	2.0×10^{-14}	5.2×10^{-7}	1.5×10^{-7}
H-RSD-4	—	—	—	47.2	8.5×10^{-14}	2.7×10^{-6}	2.0×10^{-7}
H-RSD-5	—	—	—	57.8	2.9×10^{-13}	5.9×10^{-6}	2.9×10^{-7}
Cuprophan	—	—	—	42.0	6.7×10^{-14}	1.7×10^{-6}	1.5×10^{-6}

^a H-RSD-1, 2, 3, 4, and 5 correspond to heparinized RSD-1, 2, 3, 4, and 5, respectively.

^b N.T.: Impossible to measure due to low permeability.

TABLE II
Feeding Monomer Composition, Water Content, and Permeability of RD and H-RD Membrane

Sample No.	Feeding Composition (wt %)			Water Content (wt %)	λL_p ($\text{g}^{-1} \text{cm}^3 \text{s}$)	P_2 (NaCl) ($\text{cm}^2 \text{s}^{-1}$)
	Graftmer-R ₃	SM	DAEM			
RD-1	95.2	0	4.8	10	N.T.	N.T.
RD-2	90.9	0	9.1	23	N.T.	N.T.
RD-3	85.5	0	14.5	65	8.2×10^{-13}	3.7×10^{-6}
H-RD-1 ^a	—	—	—	5.8	N.T. ^b	N.T.
H-RD-2	—	—	—	12.5	N.T.	N.T.
H-RD-3	—	—	—	19.1	N.T.	1.2×10^{-8}

^a H-RD-1, 2, and 3 correspond to heparinized RD-1, 2, and 3 respectively.

^b N.T.: Impossible to measure due to low permeability.

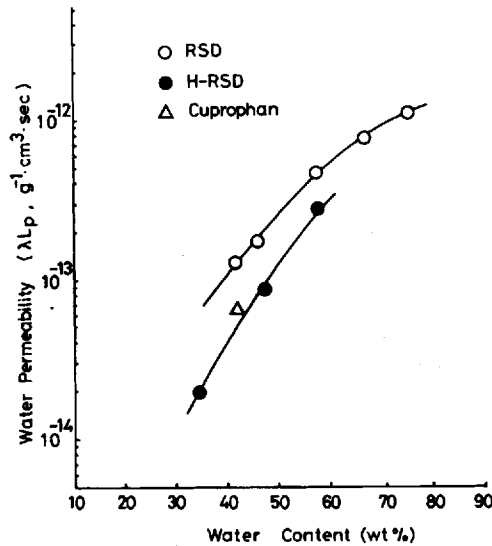


Figure 2. Dependency of water permeability (λL_p) of H-RSD (●), RSD (○) and Cuprophan (Δ) membranes upon water content.

been widely used as a hemodialysis membrane, the H-RSD-4 membrane which has similar permeabilities to that of Cuprophan was selected as the microencapsulation material for activated charcoal.

Scanning electron microscopic studies on microencapsulated activated charcoal granules: In Table III the polymer concentration of the RSD-4 solution used for the microencapsulation and the thickness of the coating layer are summarized. As shown in Table III, the thickness of the coating layer increases with the polymer concentration of the RSD-4 solution. The scanning electron micrographs of the surfaces of the uncoated charcoal granule (MC-2), the

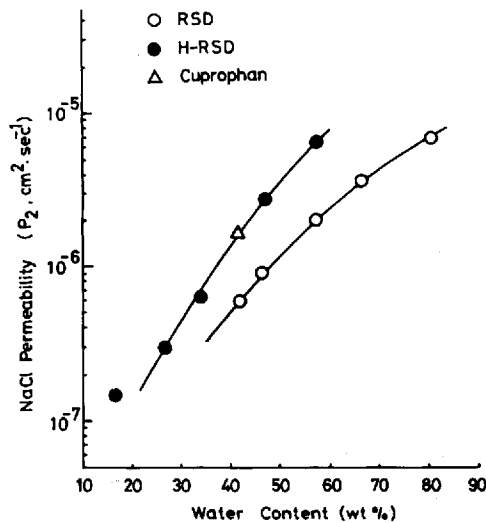


Figure 3. Dependency of NaCl permeability of H-RSD (●), RSD (○) and Cuprophan (Δ) membranes upon water content.

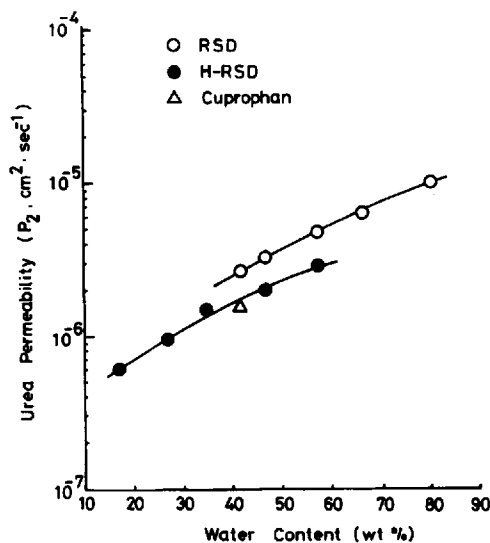


Figure 4. Dependency of urea permeability of H-RSD (●), RSD (○) and Cuprophane (Δ) membranes upon water content.

charcoal granule with a coating thickness of about $1\ \mu\text{m}$ (MC-5) and the charcoal granule with a coating thickness of about $3\ \mu\text{m}$ (MC-6) are shown in Figures 5, 6, and 7, respectively. Furthermore, the cross section of MC-6 is shown in Figure 8. These photographs reveal that the surface of the uncoated activated charcoal granules is rough and numerous fine carbon microparticles are present (Fig. 5). However, if the thickness of the coating layer is increased to about $1\ \mu\text{m}$, the fine carbon particles are completely covered by the coating layer although the surface is still rough (Fig. 6). Furthermore, when the coating layer becomes thicker (about $3\ \mu\text{m}$), the smoothness of the surface becomes fairly good (Fig. 7).

In vitro adsorption studies: Stirred batch adsorption studies were performed using creatinine and uric acid as adsorbates and the uncoated activated charcoal granules (MC-2) and granules with a coating thickness of about $1\ \mu\text{m}$ (MC-4). The creatinine adsorption curves of MC-2 and MC-4 are shown in Figure 9, indicating that there is not a significant difference in adsorption rate of creatinine between the uncoated and coated charcoal, although the initial adsorption of the uncoated charcoal is slightly higher than that of the coated

TABLE III
Microencapsulation Conditions and Membrane Thickness

Sample No.	Charcoal Granule	Polymer Concentration (wt %)	Thickness (μm)
MC-1	MQ	—	0
MC-2	LLP	—	0
MC-3	LLP	1	<0.5
MC-4	LLP	2	ca. 1
MC-5	MQ	2	ca. 1
MC-6	LLP	4	ca. 3

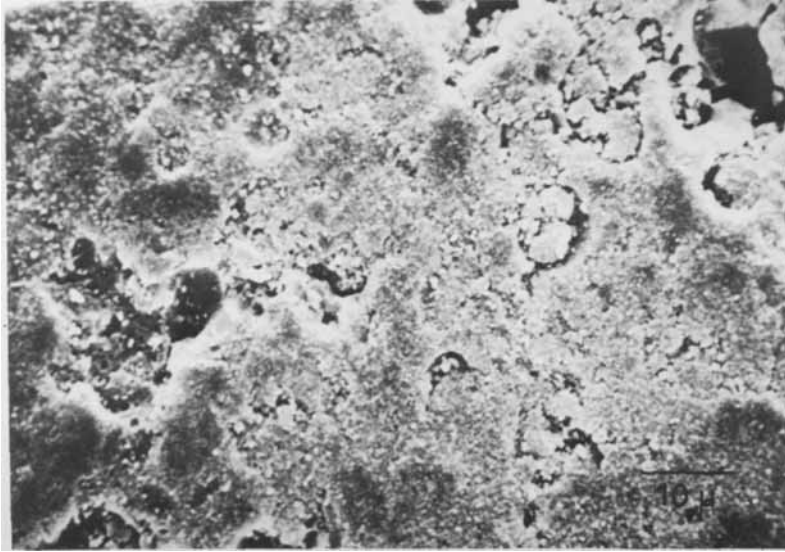


Figure 5. Scanning electron micrograph of the surface of uncoated activated charcoal granule (MC-2). The surface is rough and numerous fine carbon microparticles are observable.

charcoal. The adsorption behavior of uric acid is quite similar to that of creatinine, although the adsorption curves are not presented in this communication.

In vivo studies: Direct hemoperfusion experiments were performed using



Figure 6. Scanning electron micrograph of the surface of charcoal granule with a coating thickness of about 1 μ (MC-5). The surface is still rough, while fine carbon particles are covered by the coating layer.



Figure 7. Scanning electron micrograph of the surface of charcoal granule with a coating thickness of about 3 μm (MC-6). The surface is completely smooth.

the uncoated activated charcoal granules (MC-1) and granules with a coating thickness of about 1 μm (MC-5). Figure 10 shows the increase in the pressure drop between the inlet and outlet of the charcoal cartridge during the hemoperfusion, indicating that with the uncoated charcoal, ΔP rapidly rose to more

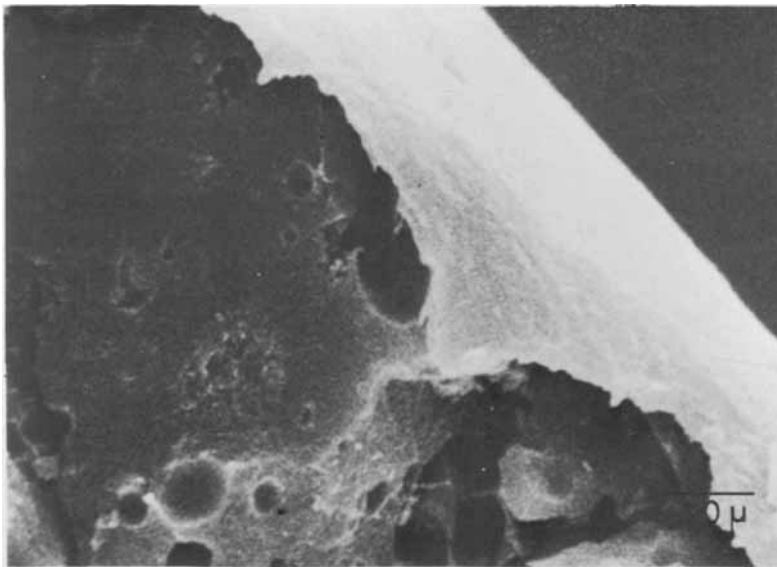


Figure 8. Scanning electron micrograph of the cross section of the coated activated charcoal granule (MC-6).

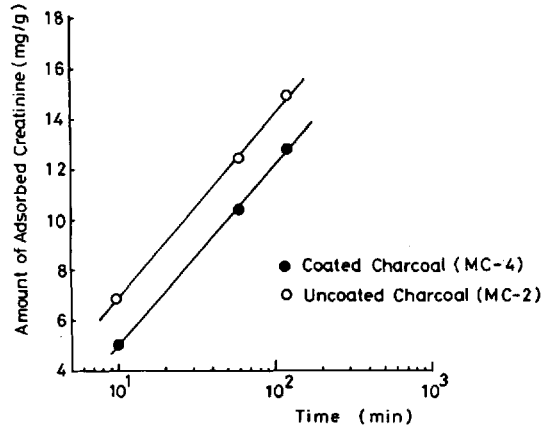


Figure 9. In vitro creatinine adsorption curves of uncoated charcoal (MC-2) (O) and coated charcoal (MC-4) (●).

than 150 mmHg for approximately 30 min, while with the coated charcoal ΔP gradually increased. Large red clots were observed in the cartridge of the uncoated charcoal after 30 min hemoperfusion, while in the coated charcoal no red clot was formed.

The curves of the creatinine concentration in blood are shown in Figure 11. In the case of the uncoated charcoal, the hemoperfusion could not be continued for more than 30 min due to the markedly increased pressure drop caused by the clot formation.

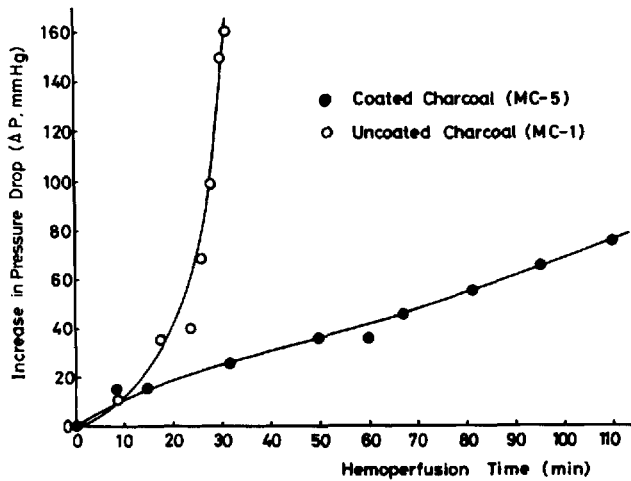


Figure 10. Pressure drop (ΔP) between the inlet and outlet of charcoal cartridge during direct hemoperfusion using uncoated charcoal (MC-1) (O) and coated charcoal (MC-5) (●). In the uncoated charcoal, the hemoperfusion could not be continued for more than 30 min due to the markedly increased pressure drop.

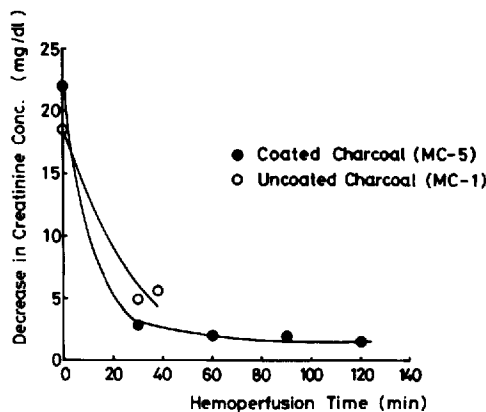


Figure 11. The curves of creatinine in blood during direct hemoperfusion using uncoated charcoal (MC-1) (O) and coated charcoal (MC-5) (●). In the uncoated charcoal, the hemoperfusion could not be continued for more than 30 min due to the markedly increased pressure drop.

DISCUSSION

The most important characteristic of the heparinized hydrophilic polymer (H-RSD) is that this polymer is composed of three elements which play the following roles, respectively; the hydrophobic element (Graftmer R₃: copolymer composed of vinylchloride, ethylene and vinylacetate) provides the mechanical strength of the H-RSD polymer, the nonionic hydrophilic element [SM: methoxypoly(ethyleneglycol methacrylate)] controls the water content of the H-RSD polymer and the cationic element (DAEM: quaternized dimethylaminoethyl methacrylate) controls the amount of heparin bound to the polymer.

As previously reported,^{3,6} the nonionic hydrophilic element (SM) is very important in controlling the rate of heparin release from the H-RSD surface into the blood stream, leading to excellent blood compatibility. Simultaneously, this hydrophilic element also plays an important role in the permeability. Figure 12 shows the decrease in the water content by heparinization. In the RSD membrane with the nonionic hydrophilic element (SM), the reduction in the water content by heparinization is minimized, although the water content of the RD membrane without SM is significantly reduced by heparinization, especially in the region of high water content of the RD membrane.

These findings suggest that the cationic element (quaternized dimethylaminoethyl methacrylate) of the RSD and RD polymers is highly hydrophilic but once ionic complex is formed between the quaternized amine groups of the RSD and RD polymers and the sulfonate groups of heparin, the cationic element loses its hydrophilicity. Consequently, in order to maintain a moderate water content for appropriate permeability after heparinization, the introduction of the nonionic hydrophilic element (SM) is considered to be crucial.

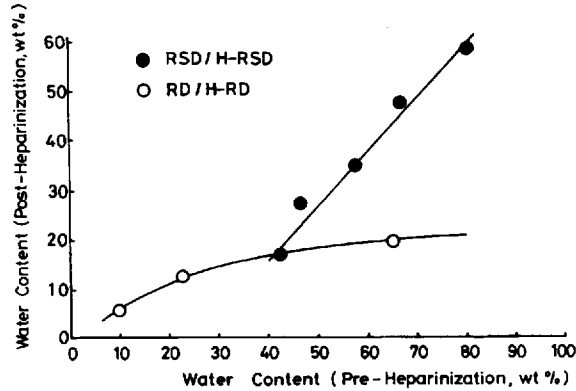


Figure 12. The reduction in water content of the RSD membrane (●) with nonionic hydrophilic element (SM) and RD membrane (○) without SM by heparinization. The reduction is significantly greater in the RD membrane than in the RSD membrane.

On the other hand, Figure 13 shows the decrease in the NaCl permeability of the RSD and RD membrane by heparinization, indicating that the introduction of the nonionic hydrophilic element effectively prevents the reduction in the NaCl permeability. This reduction in permeability results from the reduction in the water content provided by the heparinization. In addition, as shown in Tables II and III, similar effects are evident in the water permeabilities of the H-RSD and H-RD membranes.

Therefore, good permeability can not be achieved unless the nonionic hydrophilic element is introduced into the heparinized membrane.

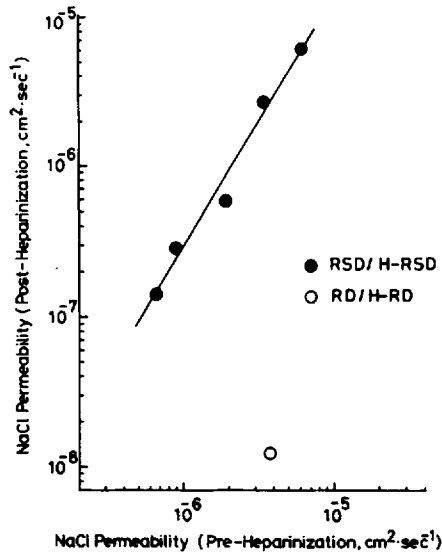


Figure 13. The reduction in NaCl permeability of the RSD membrane (●) with nonionic hydrophilic element (SM) and RD membrane (○) without SM by heparinization. The reduction is significantly greater in the RD membrane than in the RSD membrane.

As shown in Figures 2, 3, and 4, the H-RSD membrane shows a higher NaCl permeability and lower water and urea permeabilities as compared to the RSD membrane. We have previously demonstrated that the RSD membrane has the positive membrane potential ranging from 8 to 15 mV due to the quaternized dimethylaminoethyl groups, while the H-RSD membrane has a negative membrane potential ranging from -3 to -10 mV due to the sulfonate groups of the bound heparin.⁷ The higher NaCl permeability of the negatively charged membrane (H-RSD) than that of the positively charged membrane (RSD) is considered to result from the difference between the mobilities of sodium and chloride ions in the membrane.

The H-RSD-4 membrane was selected as the microencapsulation material, since among the H-RSD membranes with varying permeabilities the H-RSD-4 membrane shows the permeability most close to that of Cuprophan. In the H-RSD-4 membrane, water, NaCl, and urea permeabilities are $8.5 \times 10^{-14} \text{ g}^{-1} \text{ cm}^3 \text{ s}$, $2.7 \times 10^{-6} \text{ cm}^2 \text{ s}^{-1}$ and $2.0 \times 10^{-6} \text{ cm}^2 \text{ s}^{-1}$, respectively, and in Cuprophan the corresponding permeabilities are $6.7 \times 10^{-14} \text{ g}^{-1} \text{ cm}^3 \text{ s}$, $1.7 \times 10^{-6} \text{ cm}^2 \text{ s}^{-1}$ and $1.5 \times 10^{-6} \text{ cm}^2 \text{ s}^{-1}$, respectively.

As shown in Figure 9, there is no significant difference in the adsorption rates of the uncoated and coated charcoal, since the inclination of adsorption curve of coated charcoal is similar to that of uncoated charcoal. This suggests that the H-RSD-4 coating layer is permeable to creatinine and uric acid and that the adsorptive sites of the charcoal are not impaired by the current microencapsulation procedure. In the activated charcoal coated with the H-RSD-4 membrane, on initial retardation in adsorption due to the diffusion of the adsorbate across the coating layer is observed.

The *in vivo* adsorptive capacity of the coated charcoal is slightly enhanced compared to the uncoated charcoal, suggesting that H-RSD coating layer prevents packing, clumping and channeling by preventing clot formation and caking (Fig. 11). In the coated charcoal, the increase in the pressure drop between the inlet and outlet of the charcoal cartridge is about 20 mmHg for 30 min hemoperfusion, while in the uncoated charcoal, the increase in the pressure drop reaches to about 150 mmHg for about 30 min and the perfusion cannot be continued (Fig. 10). This means that H-RSD coating layer effectively prevents the clot formation induced by the blood contact with the charcoal surface.

It is concluded that H-RSD polymer is a promising microencapsulation material for direct hemoperfusion or hemodialysis membranes. This is due to the good permeability and the thromboresistance of the H-RSD polymer.

References

1. E. W. Merrill, E. W. Salzman, B. J. Lipps, Jr., E. R. Gilliland, W. G. Austen, and J. Joison, "Antithrombogenic Cellulose Membranes for Blood Dialysis," *Trans. Amer. Soc. Artif. Internal Organs*, **12**, 139-150 (1966).
2. I. O. Salyer, G. L. Ball III, and G. L. Beemsterboer, "The Monsanto Polyacrylonitrile Hollow-Fiber Artificial Kidney," *J. Biomed. Mater. Res.* **6**, 59-79 (1972).

3. H. Tanzawa, Y. Mori, N. Harumiya, M. Hori, N. Oshima, and Y. Idezuki, "Preparation and Evaluation of a New Athrombogenic Heparinized Hydrophilic Polymer for Use in Cardiovascular System," *Trans. Am. Soc. Artif. Internal Organs*, **19**, 188-194 (1973).
4. Y. Idezuki, H. Watanabe, M. Hagiwara, K. Kanasugi, Y. Mori, S. Nagaoka, M. Hagio, I. Yamamoto, and H. Tanzawa, "Mechanism of Antithrombogenicity of a New Heparinized Hydrophilic Polymer: Chronic in vivo Studies and Clinical Application," *Trans. Am. Soc. Artif. Int. Organs*, **21**, 436-448 (1975).
5. Y. Mori, S. Nagaoka, Y. Masubuchi, M. Itoga, H. Tanzawa, T. Kikuchi, Y. Yamada, T. Yonaha, H. Watanabe, and Y. Idezuki, "The Effect of Released Heparin from the Heparinized Hydrophilic Polymer (H-RSD) on the Process of Thrombus Formation," *Trans. Am. Soc. Artif. Intern. Organs*, **24**, 736-744 (1978).
6. Y. Mori, S. Nagaoka, M. Itoga, H. Tanzawa, Y. Yamada, H. Watanabe and Y. Idezuki, "The Effect of Heparin Release from a Heparinized Hydrophilic Polymer (H-RSD) on Antithrombogenicity," *Artif. Organs*, **2** (Suppl), 66-70 (1978).
7. H. Miyama, N. Haurmiya, Y. Mori, and H. Tanzawa, "A New Antithrombogenic Heparinized Polymer," *J. Biomed. Mater. Res.*, **11**, 251-265 (1977).

Received April 10, 1981

Accepted July 24, 1981